Sensitivity Analysis of Controlled-Temperature Thermoresistive-based Radiometers

Savio A. Oliveira, Viviane S. G. M. Tenorio, Raimundo C. S. Freire
Electrical Engineering Department
Federal University of Campina Grande
Campina Grande, Brazil
{savio.oliveira, viviane.martins}@ee.ufcg.edu.br, rcsfreire@dee.ufcg.edu.br

***Abstract*—Currently, renewable energy is being explored all around the world. From wind, to solar radiation, many solutions are currently available on the market and many more are being developed in industry and academy. In this scenario, a thermoresistive-based radiometer would provide information regarding solar radiation to solar energy systems at a very low cost. In this paper, the sensitivity of radiometers based on thermoresistive sensors using the principle of electrical equivalence are analyzed. It is verified that the change of the temperature of the environment affects considerably its sensitivity. Another architecture was proposed in which the difference of temperature between the sensor and the environment is made constant. Here, we propose the most efficient difference of temperature in order to provide best sensitivity-wise measurements. Also, both architectures employing PTC and NTC type sensors, with analog voltage and pulse width modulated output signals, are analyzed and compared regarding their sensitivity.**

***Index Terms*—thermoresistive sensors, measurements, solar energy, radiation.**

I. Introduction

Solar radiation is composed by direct and diffused radiation, where the former is measured by pyrheliometers and the latter by radiometers. Electrical equivalence radiometers usually employs two geometrically identical sensors that are kept at the same temperature by an electrical control system. Configurations based on thermoresistive sensor using the electrical equivalence principle have been used for the measurement of physical quantities such as radiation [3]–[5], [9], [10], fluid velocity [1], [7], [8], [12] and temperature.

On a classical configuration, electrical power is applied to the sensors that are heated by the Joule effect. Variations on the sensor heating due to the incident thermal radiation, fluid velocity or the environmental temperature are compensated by equivalent variations of the electrical heating due to negative feedback control, keeping the sensor to an almost constant temperature.

The most common constant temperature configuration uses a Wheatstone bridge with the sensor in one of its arms, as shown in Figure 1(a). In this configuration, the relationship between the output signal and the input quantity is not linear. Another configuration, shown in Figure 1(b), uses a pulse width modulator on the feedback loop and has the advantage of having a linear relation between the output signal and the input quantity for the cases of measurement of radiation and temperature, besides allowing a direct conversion of the input signal to voltage on the digital form [2], [9], [11], [13].

In this paper its proposed an analysis of the equivalence radiometer configuration where the temperature difference between the sensor and environment is kept constant and the classical constant temperature architecture. The classical and the proposed architectures are analyzed, considering PTC and NTC sensors, and analog and pulse width modulated output voltage. It is shown that the Constant Difference of Temperature architecture presents better performance with respect to the sensitivity when compared to the classical one.

II. Theoretical Background

The Wheatstone bridge electric equivalence radiometer employing a PTC sensor is shown in Figure 1(a) for the analog output and Figure 1(b) for the pulsed output. On Figure 1(b) it is also present the representation of the pulse width modulated (PWM) output voltage, where E and P are constant, representing the pulse amplitude and the period, respectively, τ is the pulse duration, and the duty cycle can be calculated by $D = \tau/P$.

The effective RMS voltage applied to the Wheatstone bridge for the PWM architecture is then $E\sqrt{D}$. The PTC sensor is heated by the electric power delivered by the feedback effective voltage and increases resistance with temperature. In steady state, the PTC temperature stabilizes to a value above the ambient temperature, defined by the values of the fixed resistors.

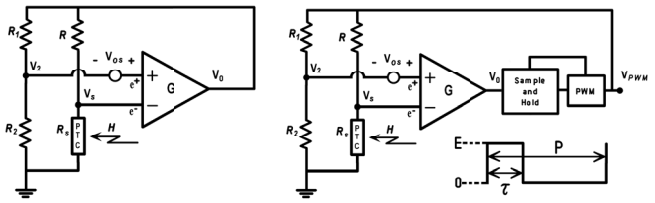

(a) (b)

Fig. 1. (a) Architecture using PTC and analog output. (b) Architecture using PTC and pulsed output with pulse width representation.

An increase in the incident radiation tends to increase the sensor temperature, but it is compensated by the Wheatstone bridge feedback circuit, which decreases the effective output voltage and the electric power delivered to the sensor. In a similar way, a decrease of incident radiation is compensated by an increase in the electric power delivered to the sensor.

In any case, the sensor resistance and its temperature are kept at an almost constant value. For the configurations employing a NTC sensor, which decreases its resistance with the temperature, the sensor arm of the bridge is connected to the operational amplifier positive input (instead of the negative input, as for the PTC sensor).

The Constant Sensor Temperature (CT) Radiometer Architecture is shown on Figure 1(a), using the first law of thermodynamics applied to the sensor, in steady state, one has:

$$\alpha SH + \frac{{V_s}^2}{R_s} = US(T_s - T_a) \tag{1}$$

Where H is the incident radiation on the sensors surface, S is the area exposed to the radiation, α is the absorption coefficient, U is the overall heat transfer coefficient, T_s is the sensor temperature and T_a the environment temperature. For a thermoresistive sensor of the PTC type, its resistance as function of its temperature is given by:

$$R_s \approx R_0(1 + \beta T_s) \tag{2}$$

Where R_0 is the resistance of the sensor at $0°C$ and β is its temperature coefficient. For a thermoresistive sensor of the NTC type, the relationship between its resistance and its temperature is given approximately by:

$$R_s \approx R_\infty e^{B/T_s} \tag{3}$$

Where R_∞ is the resistance of the sensor as the temperature tends to infinity and B is its temperature coefficient.

Considering the amplifier offset voltage negligible and making $k = (R_1 + R_2)/R_1$, the relationship between the sensor RMS voltage and the bridge applied voltage for the circuits of Figure 1(a) and 1(b) are given, respectively by:

$$V_s = \frac{V_o}{k} \tag{4}$$

and

$$V_s = \frac{E\sqrt{D}}{k} \tag{5}$$

Choosing resistors R_1 and R_2 to be equal, equations 4 and 5 can be written as:

$$V_s = \frac{V_o}{2} \tag{6}$$

and

$$V_s = \frac{E\sqrt{D}}{2} \tag{7}$$

Thus, from parameters presented in Table I, simulations based on this principle were performed comparing two main architectures: Constant Temperature (CT) and Constant Difference of Temperature (CDT).

A. Constant Sensor Temperature Radiometer Architecture

For the Constant Temperature (CT) architecture, the sensor is heated to a certain temperature and radiation can be measured upon the difference of temperatures between room temperature and sensor temperature. This was proposed in [6] and has been proven to be a good approach regarding accuracy to anemometers.

In this case, same idea will be used to evaluate radiation measurement.

From (1) the bridge voltage can be expressed for every combination of the configurations of Figure 1 and sensor type: for the analog voltage output (4) and PTC (2), yields expression (8), and for the NTC (3), yields (9); for the pulsed voltage output (5) and PTC (2), yields expression (10), and for the NTC (3), yields (11):

$$V_o = k\sqrt{R_0(1 + \beta T_s)[US(T_s - T_a) - \alpha SH]} \tag{8}$$

$$V_o = k\sqrt{R_\infty e^{B/T_s}[US(T_s - T_a) - \alpha SH]} \tag{9}$$

$$D = \frac{k^2}{E^2}\left[R_0(1 + \beta T_s)[US(T_s - T_a) - \alpha SH]\right] \tag{10}$$

$$D = \frac{k^2}{E^2}\left[R_\infty e^{B/T_s}[US(T_s - T_a) - \alpha SH]\right] \tag{11}$$

In order to evaluate the dependence of the configurations output signal (V_o or D) with the environment temperature, simulations were made for T_a varying from -20 to $40°C$ and several values of the incident radiation, with sensor parameters given in Table I, and with the $k = 2$. Figure 3(a) presents voltage output response for the CT configuration for NTC sensor and Figure 3(c) the same analysis for the PTC sensor.

TABLE I
PARAMETERS USED ON SIMULATIONS.

Simulation parameters		
Both sensors	α	0.9
	U	$211.5\,WC°/m^2$
PTC sensor	S	$2.00 \cdot 10^{-5}\,m^2$
	β	$0.00385\,°C^{-1}$
	R_0	$100\,\Omega$
NTC sensor	S	$2.46 \cdot 10^{-5}\,m^2$
	B	$3468\,K$
	R_0	$200\,\Omega$

Given the maximum output voltage visualized in Figures 3(a) and 3(c), one can choose a controlled voltage $E = 11.9\,V$ for the PTC sensor and $E = 6.4\,V$ for the NTC sensor.

Therefore, the PWM architecture was normalized for both sensors. The output for the pulse-width configuration is presented in Figure 3(b) for the NTC sensor and in Figure 3(d) for the PTC sensor.

It's seen that the increase in room temperature decreases the output voltage in both architectures. This calls to a limitation, specially in use cases where there is a high solar incidence and high temperatures (above 30 $°C$). Usually, devices facing

the sun for solar radiation measurement are likely to have their temperature rising over 30°C. This is the main motivation for architecture with Constant Difference of Temperature, which will be detailed in the next section.

B. Constant Difference of Temperature Radiometer Architecture

One alternative architecture to the circuits on Figure 1 is presented on Figure 2.

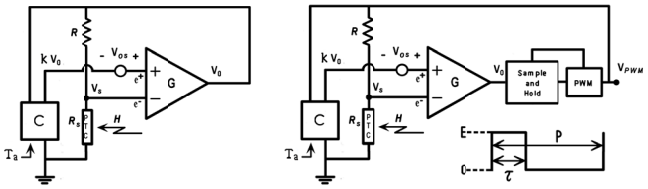

(a) (b)

Fig. 2. (a) Constant temperature difference architecture using PTC and analog output. (b) Constant temperature difference architecture using PTC with pulse width representation.

In this one, the control block C is used to generate a kV_o (or kV_{PWM}) output in order to make constant the difference between the temperatures of sensor and the environment. As an input of the controller block C, theres the bridge output voltage and also the environment temperature T_a. From the expressions (8) to (11) expression can be found in cases where the temperature difference between the sensor and the fluid is constant, which are presented on the expressions from (12) to (15) for the architectures with PTC and analog output, with NTC and analog output, with PTC and pulsed output and with NTC and pulsed output, respectively.

$$V_o = \frac{1}{k}\sqrt{R_0(1+\beta T_s)[US\Delta T - \alpha SH]} \tag{12}$$

$$V_o = \frac{1}{k}\sqrt{R_\infty e^{B/T_s}[US\Delta T - \alpha SH]} \tag{13}$$

$$D = \frac{1}{k^2E^2}\left[R_0(1+\beta T_s)[US\Delta T - \alpha SH]\right] \tag{14}$$

$$D = \frac{1}{k^2E^2}\left[R_\infty e^{B/T_s}[US\Delta T - \alpha SH]\right] \tag{15}$$

In order to evaluate the dependence of the input (V_o or τ/P) with the environment temperature (T_a), the graphs from Figure 4 were drawn. It was found from the expressions (12) to (15), for a positive and real quantity output, where $US\Delta T$-$\alpha SH \geq 0$. The same output analysis was made for the CDT architecture. It was found that the PTC sensor requires a minimum difference of temperature in the maximum radiation case to provide an output. The same does not occur for the NTC sensor, since it provides output for very little differences between sensor and room temperatures.

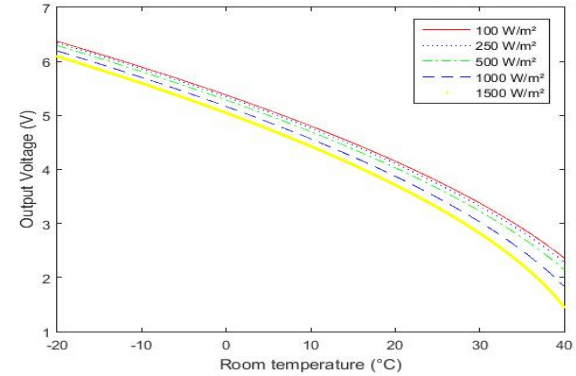

(a) Radiometer Constant Temperature: NTC Analog Output Dynamics

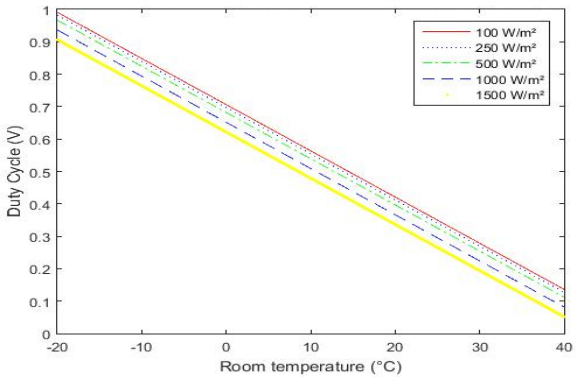

(b) Radiometer Constant Temperature: NTC Pulse-Width Output Dynamics

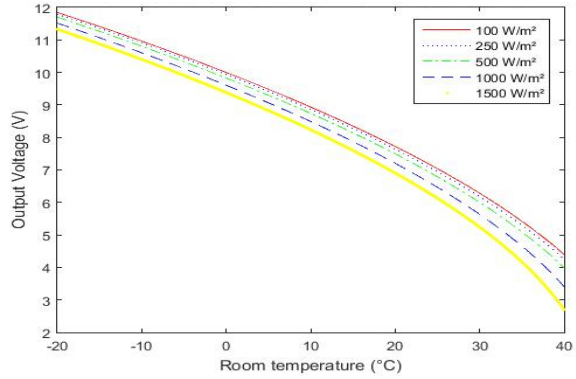

(c) Radiometer Constant Temperature: PTC Analog Output Dynamics

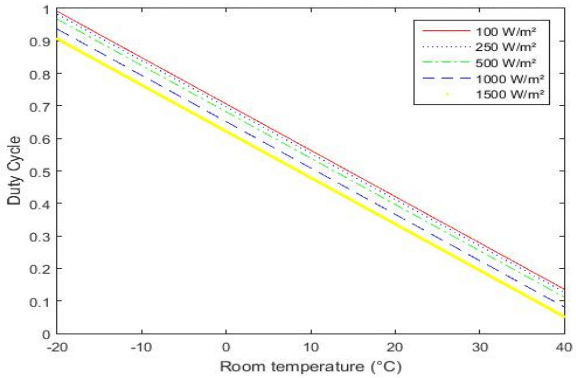

(d) Radiometer Constant Temperature: PTC Pulse-Width Output Dynamics

Fig. 3. Radiometer constant temperature outputs dynamics.

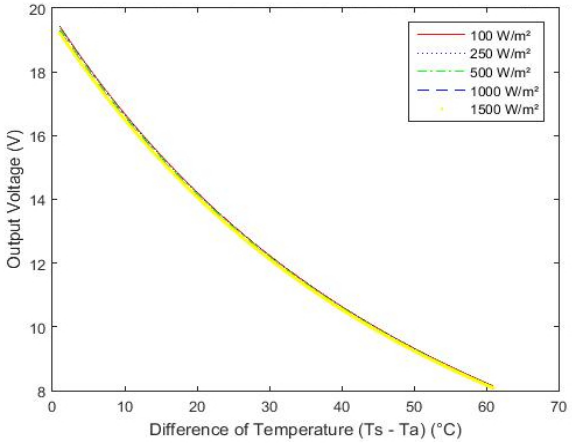

(a) Radiometer Constant Difference of Temperature: NTC Analog Output

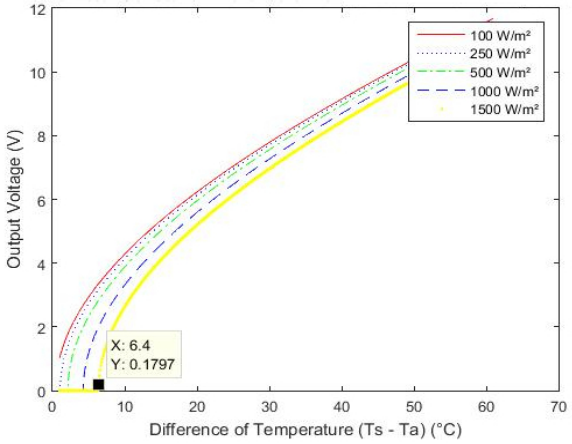

(b) Radiometer Constant Difference of Temperature: PTC Analog Output

Fig. 4. Radiometer constant difference of temperature outputs.

For the maximum radiation considered $(1500\,W/m^2)$ and with the parameters of the chosen sensor, its found that $\Delta T \geq 6.38°C$. Therefore, the minimum difference of temperature used on the next simulations was $\Delta T = T_s - T_a = 7°C$.

Comparing the graphs from Figure 4 with the ones from Figures 3(a) to 3(d), its possible to verify that the output quantity on the architectures with the constant difference of temperature are way less dependent of the room temperature, overcoming the issue with the previous architecture. In the CT architecture, the greater the room temperature, the smaller output voltage for the NTC sensor. On the other hand, for the NTC sensor in the CDT architecture, even for high room temperatures, output voltage is greater than 8 V, making this architecture more suitable for a real implementation.

From the expressions (12) to (15) were found the expressions from (18) to (21) for the relative sensitivities for the architecture PTC and analog output, with NTC and analog output, with PTC and pulsed output and with NTC and pulsed output, respectively. It was chosen the value $E = 11.9\,V$, which is a little bit higher than the maximum value of the output voltage for the PTC, and $E = 19.5\,V$ for the NTC.

III. Sensitivity Analysis

A. CT Architecture

In order to evaluate sensitivity, one has:

$$\frac{\delta V_o/V_{omax}}{\delta H/H_{max}} = \frac{-\alpha H_{max}}{2\sqrt{US(T_s-T_a)-\alpha SH}\sqrt{US(T_s-T_a)-\alpha SH_{min}}} \tag{16}$$

Also,

$$\frac{\delta D/D_{max}}{\delta H/H_{max}} = -\frac{\alpha H_{max}}{U(T_s-T_{amin})+\alpha H_{min}} = cte. \tag{17}$$

Sensitivity can be obtained from:

$$\frac{\delta V_o/E}{\delta H/H} = -\frac{\alpha SH}{2kE}\sqrt{\frac{R_0(1+\beta T_s)}{US(T_s-T_a)-\alpha SH}} \tag{18}$$

$$\frac{\delta V_o/E}{\delta H/H} = -\frac{\alpha SH}{2kE}\sqrt{\frac{R_0 e^{B(\frac{1}{T_s}-\frac{1}{T_0})}}{US(T_s-T_a)-\alpha SH}} \tag{19}$$

$$\frac{\delta \tau/P}{\delta H/H} = -\frac{\alpha SH}{k^2E^2}(R_0(1+\beta T_s)) \tag{20}$$

$$\frac{\delta \tau/P}{\delta H/H} = -\frac{\alpha SH}{k^2E^2}(R_0 e^{B(\frac{1}{T_s}-\frac{1}{T_0})}) \tag{21}$$

From equations above, sensitivity charts were obtained and can be found in Figure 5(a) to 5(d).

For this architecture, it's seen that, for both sensors, the sensitivity decreases with the increase of radiation in the analog output analysis and does not depend on room temperature for the PWM output. Moreover, for the analog output, sensitivity declines right after room temperature for any radiation above 200 W/m^2.

These are limitations of the CT architecture that are not present in the CDT architecture.

B. CDT Architecture

In an analogous way, sensitivity expressions were obtained for both sensors and both outputs (PWM and analog).

$$\frac{\delta V_o/E}{\delta H/H} = -\frac{\alpha SH}{2kE}\sqrt{\frac{R_0[1+\beta(\Delta T+T_a)]}{US\Delta T-\alpha SH}} \tag{22}$$

$$\frac{\delta V_o/E}{\delta H/H} = -\frac{\alpha SH}{2kE}\sqrt{\frac{R_0\exp\left[B\left(\frac{1}{(\Delta T+T_a)}-\frac{1}{T_0}\right)\right]}{US\Delta T-\alpha SH}} \tag{23}$$

$$\frac{\delta \tau/P}{\delta H/H} = -\frac{\alpha SH}{k^2E^2}R_0[1+\beta(\Delta T+T_a)] \tag{24}$$

$$\frac{\delta \tau/P}{\delta H/H} = -\frac{\alpha SH}{k^2E^2}R_0\exp\left[B\left(\frac{1}{(\Delta T+T_a)}-\frac{1}{T_0}\right)\right] \tag{25}$$

Figures from 6(a) to 6(d) presents the sensitivity analysis for both sensor types and architectures.

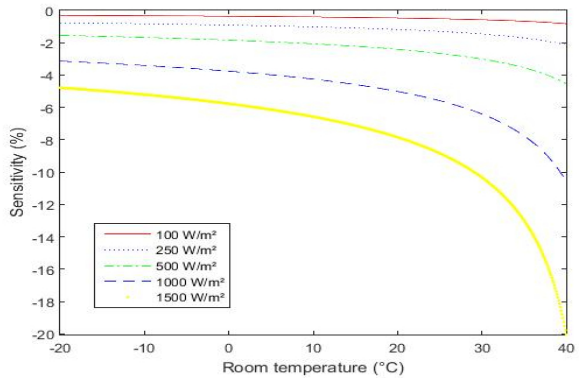

(a) Radiometer Constant Temperature: Sensitivity NTC - Analog

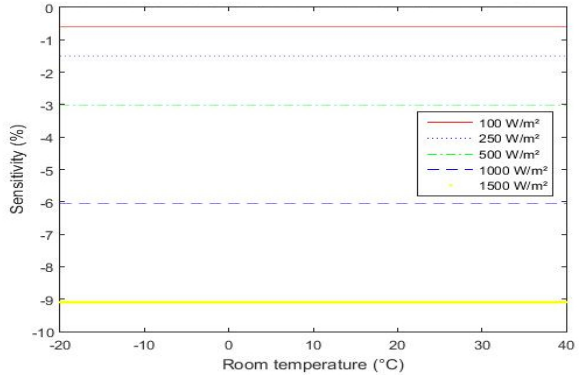

(b) Radiometer Constant Temperature: Sensitivity NTC - Pulse-Width

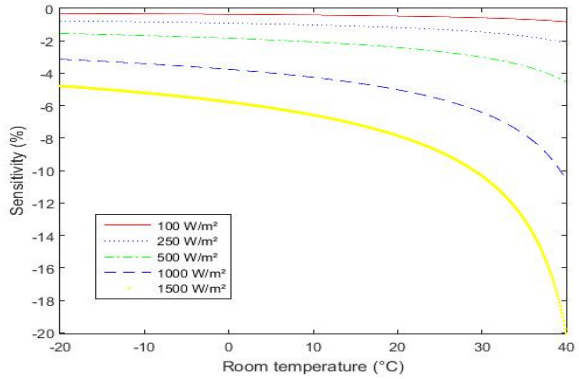

(c) Radiometer Constant Temperature: Sensitivity PTC - Analog

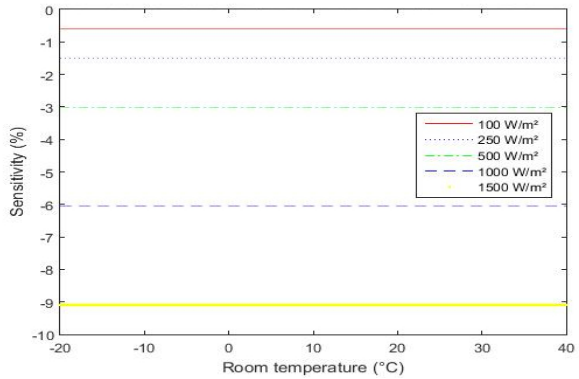

(d) Radiometer Constant Temperature: Sensitivity PTC - Pulse-Width

Fig. 5. Radiometer constant temperature sensitivities.

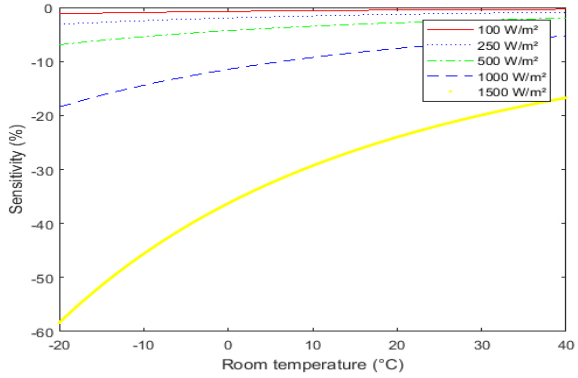

(a) Constant Difference of Temperature: Sensitivity NTC - Analog

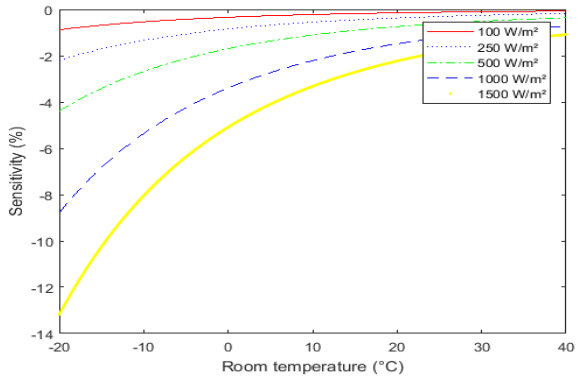

(b) Constant Difference of Temperature: Sensitivity NTC - Pulse-Width

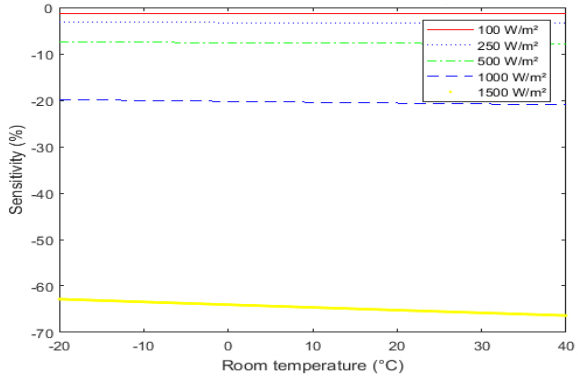

(c) Constant Difference of Temperature: Sensitivity PTC - Analog

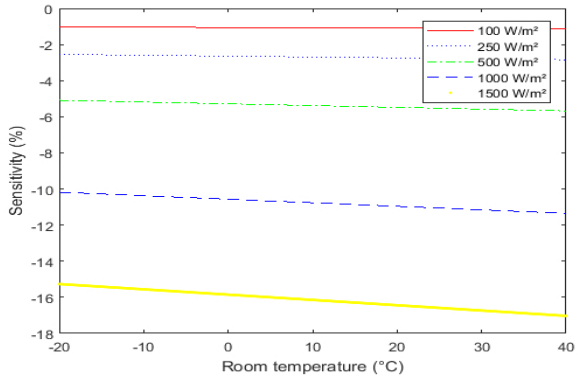

(d) Constant Difference of Temperature: Sensitivity PTC - Pulse-Width

Fig. 6. Radiometer constant difference of temperature sensitivities.

In this case, the difference of temperature (from room to sensor) is kept constant and therefore, it's independent from room temperature itself. As long as the difference is kept around 7°C, an accurate measurement can be achieved. Also, it is seen that the sensibility of the PWM architecture is linear for the PTC configuration whereas is non-linear for the NTC.

IV. Conclusions

The circuit on Figure 1 was used to evaluate the sensitivity of the radiometer with a sensor heated to a constant temperature. It was noticed that the sensitivity of the circuit with constant difference of temperature was higher compared to the four simulated possibilities: PTC sensor and analog output, PTC sensor and PWM output, NTC sensor and analog output and NTC sensor and PWM output.

The CDT architecture presented an improvement when compared to classical CT architecture due to its independence to the room temperature.

Sensitivity analysis indicates that only architecture with PTC sensor provides linear sensitivity for the PWM output.

For the sensor temperature control, the room temperature and the output of the Wheatstone bridge are inputs and the block automatically adjusts the k value. Adjusting, this way, the value of the sensor resistance and its relationship with the reference resistor R.

Acknowledgment

This research was supported/partially supported by CAPES, CNPq and NAMITEC.

References

[1] LV Araujo, SYC Catunda, CET Dórea, and RCS Freire. A controlled-temperature hot-wire anemometer with voltage feedback linearization. In *2014 IEEE International Instrumentation and Measurement Technology Conference (I2MTC) Proceedings*, pages 325–330. IEEE, 2014.

[2] G. S. Deep, J. S. R. Neto, A. M. N. Lima, R. C. S. Freire, and P. C. Lobo. Thermoresistive radiation sensor response time employing electrical heating. *IEEE Transactions on Instrumentation and Measurement*, 45(1):332–335, Feb 1996.

[3] Matthieu Denoual, D Brouard, A Veith, Olivier De Sagazan, Mathieu Pouliquen, Patrick Attia, E Lebrasseur, Y Mita, and Gilles Allègre. A heat balanced sigma–delta uncooled bolometer. *Measurement Science and Technology*, 25(6):065101, 2014.

[4] Matthieu Denoual, S Delaunay, F Durantel, B Guillet, S Lebargy, D Robbes, and J Bastie. Microbolometer on polymer membrane with heat feedback control for non radiative applications. In *Sensors, 2007 IEEE*, pages 178–180. IEEE, 2007.

[5] Matthieu Denoual, Sébastien Delaunay, and Didier Robbes. Capacitively coupled electrical substitution for bolometers. In *Sensors, 2008 IEEE*, pages 1604–1606. IEEE, 2008.

[6] RE Drubka, J Tan-Atichat, and HM Nagib. Analysis of temperature compensating circuits for hot-wires and hot-films. Technical report, Illinois Inst. of Tech. Chicago Dept. of Mechanics Mechanical and Aerospace, 1977.

[7] Romulo Pires Coelho Ferreira, Raimundo Carlos Silvério Freire, CS Deep, Jose Sérgio de Rocha Neto, and Amauri Oliveira. Hot-wire anemometer with temperature compensation using only one sensor. *IEEE Transactions on Instrumentation and Measurement*, 50(4):954–958, 2001.

[8] Romulo Pires Coelho Ferreira, Raimundo Carlos Silverio Freire, and Gurdip Singh Deep. Performance evaluation of a fluid temperature-compensated single sensor constant temperature anemometer. *IEEE Transactions on Instrumentation and Measurement*, 52(5):1554–1558, 2003.

[9] Raimundo Carlos Silvério Freire, Sebastian Yuri Cavalcanti Catunda, and Benedito Antonio Luciano. Applications of thermoresistive sensors using the electric equivalence principle. *IEEE Transactions on Instrumentation and Measurement*, 58(6):1823–1830, 2009.

[10] V. M. Nascimento, T. L. V. N. Silva, V. S. G. Martins, P. C. Lobo, and R. C. S. Freire. Output dynamic range of radiometers based on thermoresistive sensors. In *2014 IEEE International Instrumentation and Measurement Technology Conference (I2MTC) Proceedings*, pages 1271–1274, May 2014.

[11] A. Oliveira, G. S. Deep, A. M. N. Lima, and R. C. S. Freire. A feedback i/sup 2/-controlled constant temperature solar radiation meter. *IEEE Transactions on Instrumentation and Measurement*, 47(5):1163–1167, Oct 1998.

[12] Garimella R Sarma. Analysis of a constant voltage anemometer circuit. In *1993 IEEE Instrumentation and Measurement Technology Conference*, pages 731–736. IEEE, 1993.

[13] Bruno Augusto Ferreira Vitorino, Sebastian Yuri C Catunda, Diomadson Rodrigues Belfort, and Raimundo Carlos Silvério Freire. Autorange thermal sigma-delta converter for incident radiation measurement. *IEEE Transactions on Instrumentation and Measurement*, (99):1–8, 2018.